Revisiting the Measurement of Gain in Tapered Ranges

Vince Rodriguez, *Fellow*
EM Analysis Group
NSI-MI Technologies
Suwanee, GA, USA
Vince.Rodriguez@AMETEK.com

Abstract*—Tapered anechoic ranges were introduced in the late 1960s. Since their introduction tapered anechoic chambers have become popular tools for the measurement of antenna patterns at frequencies under 1 GHz. Dating back to their first installations, several papers mention the fact that these chambers did not have a spherical wave propagation and thus, the Friis transmission equation to measure gain cannot be applied [1,2]. The array factor theory of taper chambers presented in [3] states that from the point of view of the antenna in the QZ the tapered chamber appears to be a free space environment. The phase behavior across the QZ, reported in [4] appears to agree with the theory since the phase distribution follows the far field equation. In this paper simulations for a dipole and a biconical antenna are performed that suggest that the array factor theory for the tapered ranges while not perfect provides an approximated explanation for their operation. The simulations confirm the measurements done in [2] and additionally show that at some discrete frequencies the propagation in the tapered range does follow closely the free space attenuation.

I. INTRODUCTION AND BACKGROUND

It has been almost 60 years since Emerson introduced the tapered range idea [5,6]. As it was described in [3], Emerson himself did not have a clear explanation for the operation of the tapered anechoic chamber. He was aware that by bringing the specular region of the range closer to the source antenna the angles of arrival of these reflected signals were such that a very slow period occurs for the interference pattern. Thus, a very uniform illumination was created at the quiet zone (QZ). Emerson does not mention the impossibility of doing absolute gain measurements in his original paper [6] nor in his patent [5]. As early as two years after Emerson's paper engineers were studying and measuring these chambers and trying to indeed come up with a theory for their operation. In reference [2], the authors manufactured a tapered chamber scaled model that was lined with lossy foam 0.95 cm (0.375 in) in thickness (which the authors identified as Emerson & Cuming type AN-73). The chamber was a 10.79 cm (4.25 in) by 10.79 cm (4.25 in) in cross section and it is assumed that the length of the cubical section was also 10.79 cm (4.25 in). The chamber had a 24.76 cm (9.75 in) long tapered section. At the end of the tapered section there was a rectangular feed section that was 2.54 cm (1 in) by 2.54 cm by 5.08 cm (2 in) long (see Figure 1). The Authors used two "low-gain" (although the gain is not specified) E plane sectoral horns fed by a WR-90 waveguide to do their measurements of the field strength versus distance. The Authors performed measurements at 8.5 GHz and 12 GHz, with the range antenna aperture at the interface between the tapered section and the feed section as well as 2 cm (0.8 in) forward (into the tapered section) and 2 cm (0.8 in) backward (into the rectangular feed section).

While it is not mentioned implicitly on reference [2] it appears that the scaled tapered range did not have an end wall and thus the anechoic chamber was open ended.

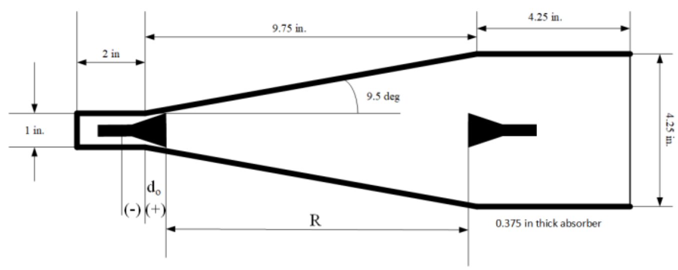

Figure 1. The scaled model of King et al. [2].

Reference [2] goes on to report reports a series of measurements that are plotted comparing the scaled tapered range field amplitude along its axis for different distances R between the two antennas to the theoretical $1/R^2$ slope and the same measurement done in free space as well as measurement done inside a scaled rectangular chamber with a 10.79 cm (4.25 in) by 10.79 cm (4.25 in) in cross section, lined with the same absorber. The results show that all the tapered measurements are between 2 and 4dB off from the free space measurement. But they are roughly parallel to the $1/R^2$ slope. The results are plotted from 5.08 cm (2 in) from the aperture to 50.8 cm (20 in) from the aperture and indeed when we approach 35.56 cm (14 in) the curves change as we are potentially outside of the tapered model, and edge diffraction from the open end becomes apparent. The results from the rectangular chamber model vary more. This can be explained by the increasing reflectivity from the walls as the test distance increases and so does the angle of incidence. Figure 2 reproduces the plots presented in reference [2].

From the results presented the authors conclude that the variations on transmission loss between the tapered chamber and the free space prevent the making of absolute antenna-gain measurements, and that a gain by substitution or reference gain antenna must be used [3]. This conclusion is repeated in [1] and the author of the present paper has heard it since he was introduced to tapered chambers early in his career. Emerson does not mention it until his 1973 paper [7], but he does not mention reference [2].

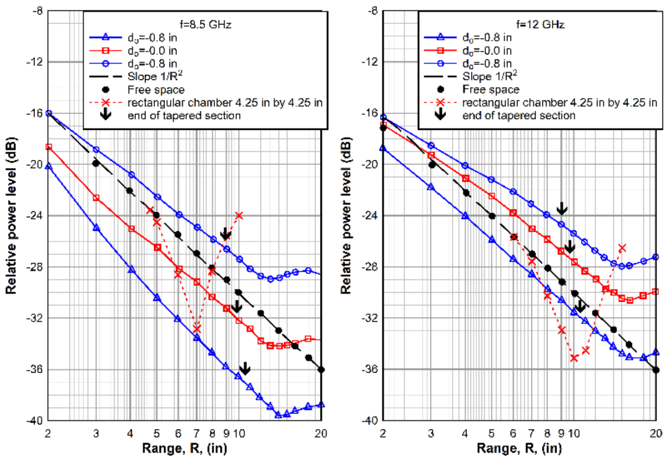

Figure 2. The results presented by King et al. [2].

II. Array Factor Theory

Reference [3] introduced the idea of the array of sources. Per this explanation of the tapered chamber operation. Per this theory, if the feed is located at the right position, the combination of small separation and attenuation of the magnitude of the elements create an array factor that is unity in amplitude and 0 degrees in phase. Essentially an array factor that is isotropic and therefore from the QZ the feed radiation will appear as if it is by itself in free space. This makes the chamber behave like a free space range. The isotropic behavior of the array factor (the 0 dB amplitude and 0-degree phase) does not have to be over the entire range of θ and φ, but only for those values of θ and φ, that encompass the QZ. This Theory explains why the positioning of the feed is critical. Any change in the electrical separation between the feed and its images will change the array factor value. It also explains why the phase of the field across the QZ tends to follow the expected behavior based on the $2D^2/\lambda$. Hence if the array factor theory is correct then potentially the gain can be computed using an approach based on the Friss transmission equation such as the two-antenna method [8].

III. Two-Antenna Method in a Tapered Range

To prove that the two-antenna method holds a model will be created. Unlike the scale model of [2] a numerical model will be used. One advantage of the numerical model is that a closer model of the RF absorber is employed. The 0.375-inch flat absorber used in [2] is a poor approach to model actual absorber as it is only 0.27λ at 8.5 GHz and 0.38λ at 12 GHz. This thickness of absorber is not a very good approximation to the typical absorber treatment on a tapered range. One of the models presented in [4] is used to perform the experiment of doing a two-antenna method gain measurement.

The chamber is a 1.52 m (5 ft) spherical QZ range having a rectangular section that is 4.88 m (16 ft) tall, 4.88 m (16 ft) wide by 8.54 m (28 ft) long with a tapered section being 9.6 m (31.5 ft) long including the feed section. The range was treated with 1.82 m (72 inch) long twisted pyramidal absorber on the end wall and 0.61 m (24 inch) long pyramidal absorber on the lateral surfaces of the rectangular section. The balance of the range was treated with 45 cm (18 inch) wedge absorber. The taper section had the 45 cm wedge trimmed down to 7.62 cm (3 inches) thickness at the interface with the feed section that was treated with 7.62 cm (3 inches) thick lossy foam block. The center of the QZ is located 3.81m (12.5 ft) from the plane where the rectangular section ends and the tapered section begins) In the center of the QZ, a dipole is positioned. The dipole is made of two cylindrical elements 15.08 cm (5.937 inches) in length and 0.106 cm (0.0416 inches) in diameter. The elements are separated by a 0.16 cm (.0628 inches) gap where a feed with a nominal 50 Ω impedance is placed. The range antenna is located 12.52 m (41.07 ft) away at the conical feed section. Figure 3 shows the model for the simulation. The simulation is done using the time domain solver of CST Suite from 100 MHz to 800 MHz. It should be noted that the dipole is intended to operate in the 400 MHz range.

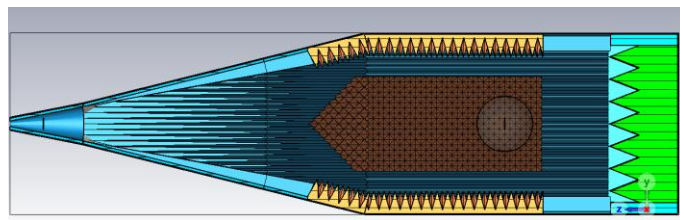

Figure 3. The model of the tapered chamber model used for the two-antenna method simulation.

IV. Numerical Results

The range is simulated and the S21 is obtained, where the S21 is the power at port 2, the feed for the dipole in the QZ related to the power at port 1, the feed port at the range antenna. Since the two antennas are identical, the Friss equation can be written as [8]:

$$\frac{P_r}{P_{in}} = G^2 \left(\frac{\lambda}{4\pi R} \right)^2 \tag{1}$$

Thus, the gain can be calculated using the following equation derived from (1),

$$G = 4\pi R \frac{\sqrt{|S_{21}|}}{\lambda} \tag{2}$$

Where all amounts in equation (2) are in linear units. From the S21 computed in the simulation, the gain obtained from the two-antenna method using equation (2). In addition to this simulation a free space simulation was conducted where the two dipoles were located using the same separation distance, but the tapered chamber was eliminated from the model. The CST model uses perfectly matched layer absorbing boundaries to terminate the finite difference computational domain. These boundaries are not perfect event when they are set to give an estimated reflection level of 10^{-6}. Thus, a similar simulation was run using a Method of Moments (MoM) package (WIPL-D). IN the WIPL-D model the two dipoles were separated by the same 12.52 m and the S21 was computed. From the S21, the gain was computed. The MoM free space simulation and the tapered chamber simulation show closer solutions at frequencies from 380 MHz to 396 MHz agree and they are closer (0.1 dB difference) than the CST free space simulation. As a check, the gain for the dipole was computed using the MoM and the FDTD approaches. The far field was computed within the software package and the gain computed. Both packages provided a computed far field (theoretically infinite distance) gain of 2.1 dB. The results of all these numerical experiments are shown in figure 4.

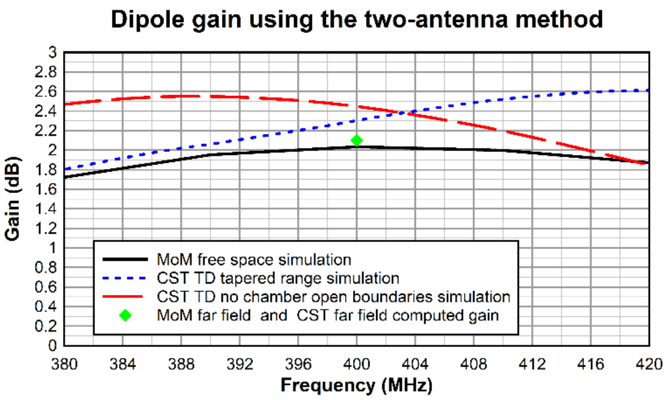

Figure 4. Results from all the simulations show good agreement at the center frequency of 400MHz.

The results show that at 400MHz, the tapered chamber simulation given a gain of 2.29 dB versus 2.447 for the CST free space simulation and 2.03 dB for the MoM free space simulation. If the 2.1dB for the far field computed gain is used for the given dipole (both FDTD and MoM results agree at 400MHz) then we can compare the results of the different simulation to these far field results. This comparison is done in Table I.

TABLE I. COMPARISON OF GAIN RESULTS

Method	Computed Gain (dB)	Computed Gain linear	Difference to far field (1.622)	% Difference
Tapered Chamber	2.29	1.6955	0.0735	4.53%
Free space FDTD	2.447	1.758	0.136	8.38%
Free space MoM	2.03	1.5983	-0.0637	-3.927%

The results for the tapered chamber simulation are not much different from the far field computed gain that the free space simulations show using two different simulation approaches.

The same analysis of the field versus distance that was done in [2] can be repeated in the simulation of the chamber at 400 MHz. In addition to the simulation with the chamber, the simulation can be repeated with the chamber, (shielding and absorber) taken out of the model leaving the source antenna in a free space domain, terminated by the matched layers used in the time domain simulations in CST Suite. Figure 5 shows the results.

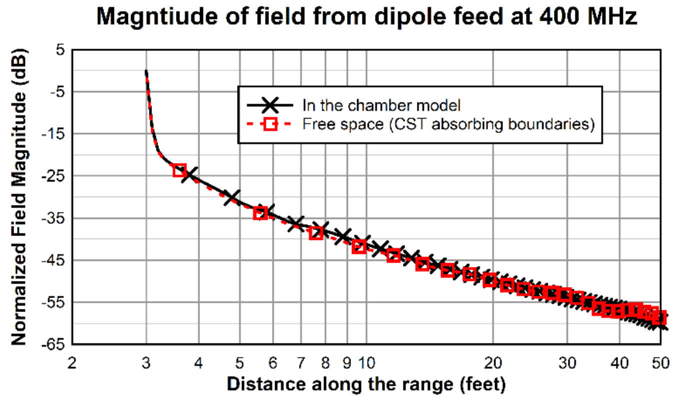

Figure 5. Normalized field distribution for the Tapered Chamber and the Free space propagation.

The data on Figure 5 show that the propagation at 400MHz in the tapered chamber is very close to the propagation in the free space model. Indeed, it looks like the perfectly match layer in the free space model has a higher reflectivity than the absorber as a standing wave is apparent from the 25 to 50 feet points. But the two sets match very well on the results. The differences in gain shown in TABLE I could be explained from other sources of error, such as reflectivity of the range.

The reflectivity of the tapered chamber simulated can be estimated from the ripple on the field sampled along a longitudinal line along the QZ. The same model used to get the dipole gain using the two-antenna method was rerun but in this case the dipole on the QZ was removed. Figure 6 shows the results of this simulation. In the QZ a ripple of ±0.125 dB is observed. This ripple corresponds to a reflectivity of about -36 dB. The period of the ripple is 40 cm (1.335 ft) which corresponds to 0.54λ at 400 MHz indicating that the direction of arrival of the interfering wave is from the back wall [9]. This ripple places a potential error of 0.125 dB on the gain measurement.

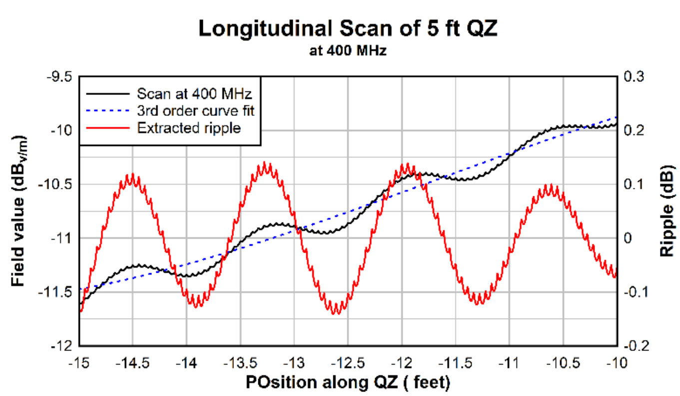

Figure 6. QZ analysis of the ripple on the longitudinal direction at 400 MHz.

V. ANALYSIS WITH A BROADER BAND ANTENNA

The simulations show that at 400MHz for the given tapered chamber the free space propagation and the propagation in the chamber follow a very similar slope and level. This seems to translate into a correct calculation for the gain using the two-antenna method. A second tapered range is analyzed. This range is a cubical section of 3.05 m (10 ft) per side with a tapered section that is 5.94 m (19.5 ft) long. The QZ of this tapered range is 1.22m from the boundary between the cubical and tapered section. The feed antenna is located 0.26 m (10 in) from the end of the tapered section. The range length is 6.91 m (272 in).

The feed antennas are biconical antennas. Each element is a truncated cone 7.62 cm (3 in) in height and with a larger base that is 8.89 cm (3.5 in) in diameter and a smaller end with a diameter of 0.254 cm (0.1 in). The elements are separated by a gap that is 0.254 cm and fed with a gap source with a 200 Ω impedance. Figure 7 shows the analyzed geometry.

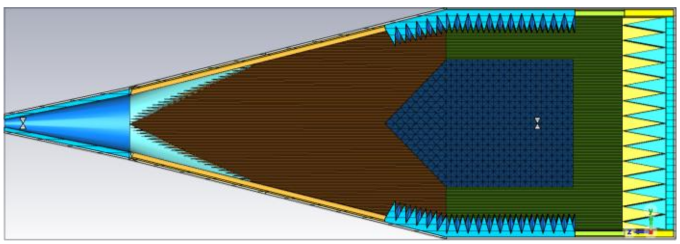

Figure 7. The second tapered model that was considered for the simulations.

The tapered range was treated with 66 cm (26 in) pyramidal absorber on the end wall and 30 cm (12 in) absorber on the lateral surfaces. The balance of the cubical section and the tapered section was treated with 7.62 cm (3 in) wedge absorber and the feed section also had 7.62 cm lossy foam block.

The same biconical antenna that is being used to feed the tapered range was placed in the center of the QZ and the S21 computed using CST time domain solver. Using equation (2) the gain was computed and compared to the Gain computed from modeling the antenna by itself. Figure 8 shows the data from these two computations. Clearly the two methods provide a very different gain except at 1.2 GHz where the two curves intersect.

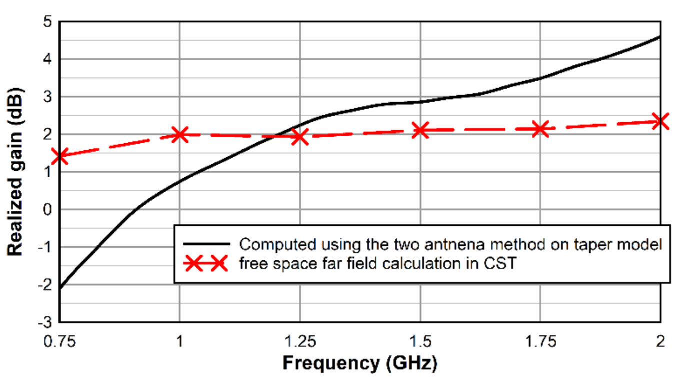

Figure 8. Computed realized gain from the simulated two antenna method in the tapered range and from the far field CST computation.

As it was done for the other chamber model at 400MHz, the field along the range from the feed to the center of the QZ is computed for the chamber (with the antenna removed form the QZ) and for a case where the chamber and absorber are removed from the model and the boundaries set to open boundaries. Figure 9 shows the results of this analysis.

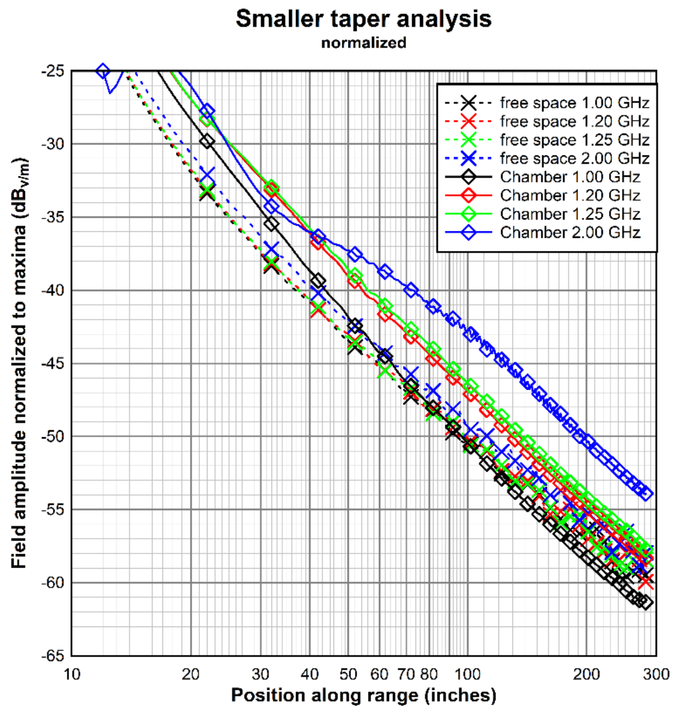

Figure 9. E field magnitude along the range length for the free space case and the tapered chamber case.

The data show that at 1 GHz and 2 GHz there is a difference between the field distributions. At 1 GHZ the difference is small but the slope of the curves is considerably different since the two curves (i.e. the free space and the tapered chamber cases at 1 GHz) cross each other around the 100 inch mark. However, at 1.2 GHz and 1.25 GHz, the slope of the curve is closer for both cases even if the difference appears to be larger.

Interestingly on the "free space calculation where the computational domain is truncated by the perfectly matched layer, a slight ripple due to numerical reflection from the boundary can be seen. A secondary computation for the same antenna geometry using the MoM (WIPL-D) was performed. Figure 10 shows the detail of these computations clearly the slope of the propagation in the chamber model is almost identical to the slope of the propagation in free space.

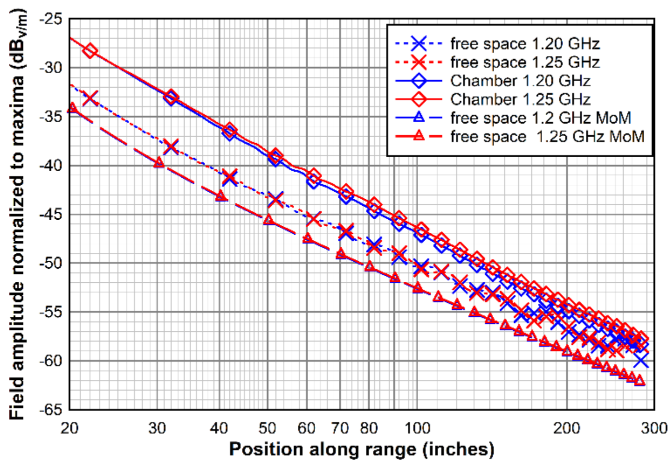

Figure 10. Detail of the field along the range for 1.2 GHz and 1.25 GHz.

If the phase is computed across the width and height of the 91.44 cm (36 inch) diameter spherical QZ, the results in Figure 11 are obtained.

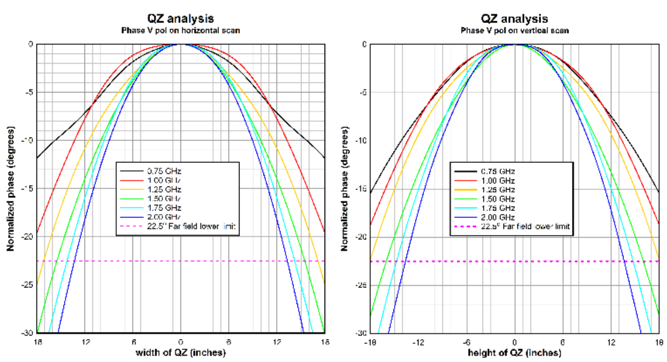

Figure 11. Phase on the QZ, notice that the 22.5 degree that is used as the far field boundary is achieved over a smaller area as frequency increases.

The span of the far field illuminated QZ can be obtained from the data in Figure 11, and it can be compared to the span obtained from the far field equation (i.e. R=[$2D^2$]/λ) where the distance is fixed to 6.91 m. The results are like what has been seen in measurements and computations and that has been reported in [3] and [4]. Figure 12 shows the different spans at which the far field lower boundary of 22.5° is achieved.

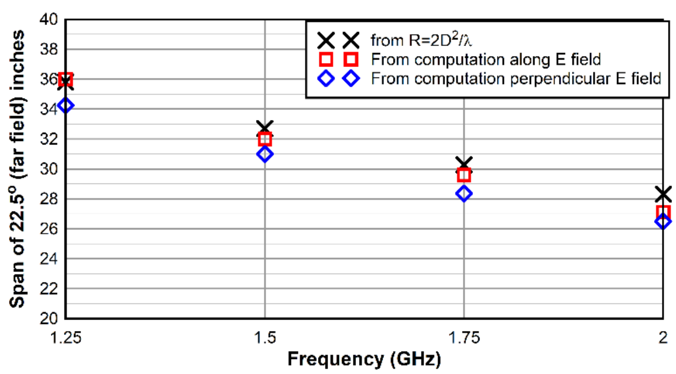

Figure 12. Span at which the far field is achieved.

VI. Conclusion

The results shown seem to invalidate the array factor theory of the taper chamber illumination. However, it must be recalled that as presented in [3] the theory was an approximation. It aims to explain the phase behavior of the tapered ranges that appear to follow the far field equation indicating a behavior like the one found in free space. The theory approximates the range to a two-dimensional structure and the array to a straight-line array.

Some of the numerical experiments do show that a method, based on free space propagation can provide the correct solution for the gain at specific frequencies. It is possible that at those frequencies, the source antenna and its images do create an isotropic array factor. It might be that at other frequencies the array factor created is not quite the isotropic ideal goal, and in those cases the behavior of the taper deviates slightly from the ideal free space.

The important thing is to remember that the tapered chambers behave in a manner that is very similar to far field ranges. That is something that both the Array Theory approximation and the Ground-Reflection-Range Theory presented in [6], appear to conclude and agree.

References

[1] W. H. Kummer and E. S. Gillespie, "Antenna Measurements _ 1978," Proceedings of the IEEE, vol. 66, no. 4, April 1978.

[2] H. E. King, F. I. Shimabukuro, J. L. Wong "Characteristics of a Tapered Anechoic Chamber" IEEE Trans. On Antennas and Prop. vol. 15, no. 3, pp. 488-490, May 1967, doi: 10.1109/TAP.1967.1138921.

[3] V. Rodriguez Anechoic Range Desing for for Electromagnetic Measurements, Artech House: Boston, Massachusets, 2019

[4] V. Rodriguez and E. Rios, "Comparison of Measurements and Simulations of Tapered Anechoic Chambers," 2022 16th European Conference on Antennas and Propagation (EuCAP), Madrid, Spain, 2022, pp. 1-5, doi: 10.23919/EuCAP53622.2022.9769196.

[5] W. H. Emerson, "Anechoic Chamber". US Patent 3,308,463, 7 March 1967.

[6] W. H. Emerson and H. B. Sefton, Jr., "An improved Design for Indoor Range," Proceedings of the IEEE, vol. 53, no. 8, pp. 1079-1081, Aug. 1965.

[7] W. H. Emerson, "Electromagnetic Wave Absorbers and Anechoic Chambers Through the Years" IEEE Trans. Ofn Antennas and Prop., Vol AP-21, No. 4, July 1973 pp. 484-490.

[8] "IEEE Recommended Practice for Antenna Measurements," in IEEE Std 149-2021 (Revision of IEEE Std 149-1977) , vol., no., pp.1-207, 18 Feb. 2022, doi: 10.1109/IEEESTD.2022.9714428.

[9] B. Tian, "Free Space VSWR Method for Anechoic Chamber Electromagnetic Performance Evaluation," in 30th Antenna Measurement Techniques Association Annual Symposium (AMTA 2008), Boston, MA, 2008.